

## Band structure of an epitaxial thin film of InSe determined by angle-resolved ultraviolet photoelectron spectroscopy

This article has been downloaded from IOPscience. Please scroll down to see the full text article.

1999 J. Phys.: Condens. Matter 11 4303

(<http://iopscience.iop.org/0953-8984/11/22/302>)

View [the table of contents for this issue](#), or go to the [journal homepage](#) for more

Download details:

IP Address: 171.66.16.214

The article was downloaded on 15/05/2010 at 11:43

Please note that [terms and conditions apply](#).

# Band structure of an epitaxial thin film of InSe determined by angle-resolved ultraviolet photoelectron spectroscopy

A Amokrane<sup>†§</sup>, F Proix<sup>†</sup>, S El Monkad<sup>†</sup>, A Cricenti<sup>‡</sup>, C Barchesi<sup>‡</sup>,  
M Eddrief<sup>†</sup>, K Amimer<sup>†</sup> and C A Sébenne<sup>†</sup>

<sup>†</sup> Laboratoire de Minéralogie–Cristallographie, UMR 7590 CNRS, case 115, Université Pierre et Marie Curie, 4 place Jussieu, 75252 Paris Cédex 05, France

<sup>‡</sup> Istituto di Struttura della Materia del CNR, via Fosso del Cavaliere 100, 00133 Rome, Italy

Received 31 December 1998, in final form 19 March 1999

**Abstract.** The valence band structure of a very thin film (about 6.4 nm thick) of the layered semiconductor InSe grown by molecular beam epitaxy onto a Si(111)1 × 1–H substrate has been determined by angle-resolved ultraviolet photoelectron spectroscopy using synchrotron radiation. The dispersion curves along the two symmetry directions of the Brillouin zone in the plane of the layers have been obtained from the angular dependence of the valence band spectra. Those along the normal to the plane of the layers have been derived from normal emission at various photon energies. It is shown that the experimental dispersion curves obtained are in very good agreement with the electronic band structure calculated for InSe bulk material of the  $\gamma$  polytype, in agreement with the crystalline structure of the film.

## 1. Introduction

InSe is a layered semiconductor of the III–VI family. The basic two-dimensional layer, 0.83 nm thick, has hexagonal symmetry, and is formed of four atomic planes in the sequence Se–In–In–Se. Bonding within the layers is ionic-covalent while the layers are bonded together by van der Waals-like interactions. Owing to these relatively weak interlayer forces, there are different stacking arrangements of the layers leading to the four polytypes  $\gamma$ ,  $\varepsilon$ ,  $\beta$  and  $\delta$  [1].

Like the other III–VI layered material GaSe [2], InSe can be epitaxially grown on Si(111) substrates [3]. In the case of GaSe, an extensive study by transmission electron microscopy (TEM) on films having a thickness in the range 8–40 nm [4, 5] has revealed that (i) films with the best crystalline quality (fewer stacking faults) are provided when grown on chemically H-passivated non-reconstructed Si(111) substrate, (ii) the lattice of the film is relaxed to its bulk parameters and (iii) the structure of the films is that of the  $\gamma$  polytype. Epitaxial thin films of InSe are expected to be also of the  $\gamma$  polytype. This is confirmed by TEM measurements on InSe/Si(111)–H interfaces [5, 6].

Concerning the electronic band structure of InSe, an experimental determination from angle-resolved photoemission on bulk material of the  $\beta$  polytype has been reported by Larsen *et al* in 1977 [7]. As far as we know, it is the only published one up to now. This work was carried out when theoretical band structures were still lacking for InSe and the authors compare their experimental dispersion curves for  $\beta$ -InSe to a theoretical band structure of

<sup>§</sup> Present address: Laboratoire de Structure et Propriétés de l'Etat Solide, Université de Lille I, 59655 Villeneuve d'Ascq Cédex, France.

$\beta$ -GaSe. At about the same time and immediately afterwards, the InSe electronic structure has motivated several theoretical investigations [8–11] because of the two-dimensional character of this layered compound. The calculations have dealt either with a single layer [8] or with the  $\beta$  and  $\epsilon$  polytypes [9–11] which have a simpler first Brillouin zone than the  $\gamma$  polytype. In particular, no electronic band structure was available in the literature for the  $\gamma$  polytype until the first principles calculation of Gomes da Costa *et al* [12] who have also calculated the band structure for  $\beta$ -InSe with the same approach.

Because of the existence of  $\gamma$  polytype in epitaxial thin films of InSe, it appeared interesting to carry out an experimental determination of the electronic band structure of such a film. Provided the film is not strained and there are no effects related to its limited thickness, comparison with results relative to bulk material will be meaningful, in particular with the experimental dispersion curves obtained by Larsen *et al* [7], and with the theoretical investigations of Gomes da Costa *et al* [12].

In this paper, we present a band structure determination for a InSe thin film grown on Si(111) $1 \times 1 - H$  by angle-resolved ultraviolet photoelectron spectroscopy (ARUPS), and low energy electron diffraction (LEED) control for orientation. We show that the experimental dispersion curves are in very good agreement with the electronic band structure calculated for InSe bulk material of  $\gamma$  polytype.

## 2. Experiment

A thin film of InSe, about 6.4 nm thick (approximately eight layers), has been grown by a molecular beam epitaxy (MBE) technique [2] onto a chemically hydrogenated non-reconstructed Si(111) $1 \times 1 - H$  substrate. The InSe film was deposited with a substrate temperature held at 430 °C and a partial pressure ratio  $P_{Se}/P_{In}$  set at about 2.3. Under these conditions, an epitaxy of the InSe compound occurs in which the layers grow parallel to the substrate surface with [10.0] InSe parallel to [1 $\bar{1}$ 0] Si as revealed by reflection high energy electron diffraction (RHEED) during growth [3]. The quality of such a film grown under similar conditions is revealed by the high resolution TEM image of figure 1 which also shows the  $\gamma$  stacking of the InSe crystallites, as well as the presence of stacking faults. The InSe crystallites have a lateral extent of about 40 nm [5] and form around 85% of the film.

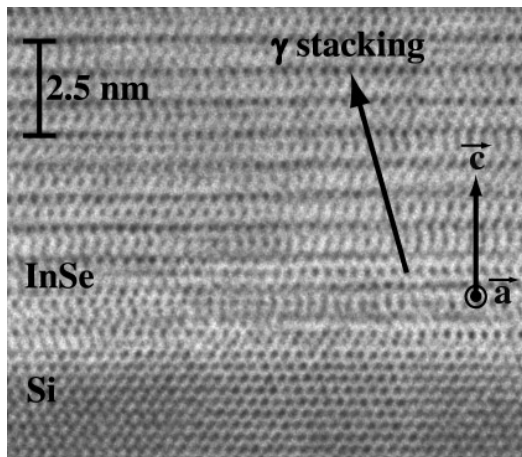


**Figure 1.** Cross section image of an InSe/Si(111)-H interface observed by high resolution transmission electron microscopy (by courtesy of A Köebel and Y Zheng).

The InSe/Si(111) sample about 0.3 mm thick was cut as a parallelepiped about  $5 \times 10 \times 0.3 \text{ mm}^3$  in size. After its preparation, the sample was kept in a desiccator under primary vacuum before being studied by ARUPS.

The measurements were performed using synchrotron radiation of the SuperACO storage ring at Laboratoire pour l'Utilisation du Rayonnement Electromagnétique (LURE) in Orsay (France) on line SA73. They were carried out under ultrahigh vacuum at a pressure of about  $1 \times 10^{-10}$  Torr. A toroidal grating with 600 lines  $\text{mm}^{-1}$ , at  $15^\circ$ , gave photons in the energy range 29–120 eV. The photoelectrons were collected with an angle-resolving hemispherical analyser rotatable around a vertical axis in the surface plane of the sample. For all the measurements, the radiation was incident upon the sample at an angle of  $22.5^\circ$  to the surface normal. All the spectra were recorded with an overall resolution of about 150 meV, which includes the monochromator and the analyser resolutions. Once under ultrahigh vacuum, the sample was outgassed at about  $200^\circ\text{C}$  in the analysis chamber, before starting the photoemission measurements.

In order to determine the dispersion curves in the plane of the layers, the valence band spectrum has been measured at various photoelectron emission angles for the two fixed photon energies of 29 and 48 eV. This study has been performed along the two symmetry directions  $\Gamma\text{M}$  and  $\Gamma\text{K}$  of the two-dimensional first Brillouin zone, corresponding respectively to the [21.0] and [10.0] directions of the real space lattice (the  $\Gamma\text{M}$  and  $\Gamma\text{K}$  directions will be specified in section 3). Along the  $\Gamma\text{M}$  direction, the spectra were taken for emission angles from  $-6^\circ$  to  $50^\circ$  and from  $-6^\circ$  to  $20^\circ$  at the photon energies of 29 and 48 eV respectively. In the  $\Gamma\text{K}$  direction, the spectra were measured for emission angles varying between  $-6^\circ$  and  $54^\circ$  and between  $-6^\circ$  and  $38^\circ$  with photons of 29 and 48 eV respectively. The spectra were recorded either at  $2^\circ$  intervals or at  $4^\circ$  intervals for those obtained in the  $\Gamma\text{M}$  direction with emission angles larger than  $10^\circ$ .

The choice of azimuth of the photoelectron emission plane, which was identical with that of the photon plane of incidence, has been achieved from the orientation of the sample by LEED control. Although the rotational symmetry of a single layer is threefold, each Se atom being bonded to three In atoms, we have assumed a sixfold symmetry, and so no distinction has been made between two azimuths separated by  $60^\circ$  from each other. The threefold local symmetry has been verified from ARUPS on InSe by Larsen *et al* [7]. These authors have indeed found that the valence band spectra obtained along the  $\Gamma\text{M}$  and  $\Gamma\text{M}'$  directions ( $\Gamma\text{M}$  and  $\Gamma\text{M}'$  forming an angle of  $60^\circ$  or  $180^\circ$ ) show considerable differences in relative intensities of peaks, but not in their energy positions. Since, for the dispersion curves determination, we are only concerned with the energy position of peaks, it is sufficient to consider a sixfold rotational symmetry.

To determine the dispersion of the electronic states along the normal to the layers, the valence band spectrum has been studied at normal emission for various photon energies between 29 and 60 eV.

Considering the photon energies used in this study, the kinetic energy of the photoelectrons excited from the valence band ranges from  $\sim 20$  to  $\sim 60$  eV. The electron escape depth of the photoelectrons, taking into account the atomic density of the material which the electrons go through [13], ranges from  $\sim 0.5$  to  $\sim 0.7$  nm. Thus, the thickest depth probed in the measurements, corresponding to normal emission, is of the order of a few InSe layers. With a 6.4 nm thick film, we expect these top layers to be relaxed to bulk InSe parameters. Indeed, Auger electron spectroscopy associated with LEED, during thermal erosion of InSe films similar to ours [14], revealed that the effect of strain on InSe is observed when the film is about 2 nm thick or thinner. In these conditions, it will be possible to compare the results reported below to those relative to bulk material.

### 3. Details of the analysis

The dispersion curves in the plane of the layers are obtained by determining the component parallel to the surface,  $k_{\parallel}$ , of the excited electron wave vector inside the solid. Using the conservation of both the energy and  $k_{\parallel}$  (without the Umklapp process) during the photoemission process, one can relate  $k_{\parallel}$  to the electron binding energy in the initial state and to the photoelectron emission angle  $\theta_e$  by the equation:

$$k_{\parallel} = [(E_i + h\nu - \Phi)2m/\hbar^2]^{1/2} \sin \theta_e. \quad (1)$$

$h\nu$  is the photon energy.  $E_i$  is the initial-state electron binding energy referred to the valence band edge  $E_{VB}$  ( $E_i \leq 0$ ). Namely,  $E_i$  is related to the photoelectron kinetic energy  $E_K(i)$  by  $E_i = E_K(i) - E_K(VB)$  where  $E_K(VB)$  is the kinetic energy of photoelectrons issued from the valence band edge. The latter  $E_{VB}$ , more precisely  $E_K(VB)$ , has been determined by linear extrapolation of the highly increasing part of the valence band spectra on the high kinetic energy side.  $\Phi$  is the ionization energy ( $\Phi > 0$ ) which corresponds to the difference between the vacuum level and the valence band edge. We have taken for the ionization energy a value of 6.08 eV determined from photoemission yield spectroscopy on a cleaved InSe bulk material [15].

To obtain the dispersion curves along the normal to the plane of the layers, one has to determine the normal component  $k_{\perp}$  of the electron wave vector inside the solid. A simple way to do this is to analyse the valence band spectra at normal emission ( $\theta_e = 0$ ) for various photon energies. Indeed, in this case, the surface parallel component of the electron wave vector inside the solid vanishes ( $k_{\parallel} = 0$ ) and so, the photoelectrons necessarily arise, inside the crystal, from electronic states depending only on  $k_{\perp}$ . Assuming a free-electron-like conduction band, the latter component can be related to the electron binding energy in the initial state by the following formula:

$$k_{\perp} = [(E_i + h\nu - \Phi - V_0)2m/\hbar^2]^{1/2}. \quad (2)$$

$V_0$  is the inner potential which corresponds to the difference between the zero of the crystalline potential and the vacuum level ( $V_0 < 0$ ). Values from the top to the bottom of the valence band are possible for the inner potential.

The dispersion relations (1) and (2) can be written in reduced units as:

$$k_{\parallel}/k_{BZ} = [(E_i + h\nu - \Phi)/E_{BZ}]^{1/2} \sin \theta_e \quad (3)$$

and

$$k_{\perp}/k_{BZ} = [(E_i + h\nu - \Phi - V_0)/E_{BZ}]^{1/2} \quad (4)$$

where  $E_{BZ} = (\hbar^2/2m)k_{BZ}^2$  is the energy of the free electron at the Brillouin zone edge.

The  $\beta$  polytype of InSe has a hexagonal unit cell containing eight atoms from two adjacent layers in which  $a$  and  $c$  are the in-plane lattice parameter and the height of one layer respectively. The first Brillouin zone is also hexagonal. It is shown in figure 2 together with the high symmetry points. The basic reciprocal-lattice vectors are  $2\Gamma M = 4\pi/a\sqrt{3} = 1.811 \text{ \AA}^{-1}$  in the plane of the layers, with  $2\Gamma M = \Gamma K\sqrt{3}$ , and  $2\Gamma A = \pi/c = 0.377 \text{ \AA}^{-1}$  perpendicular to the plane of the layers [16]. The unit cell of the  $\gamma$  polytype which contains only four atoms from one layer is rhombohedral. The three-dimensional first Brillouin zone and its contour in the  $x\Gamma z$ -plane are displayed in figures 3(a) and 3(b) respectively. Its height,  $2\Gamma Z$ , along the  $z$ -axis perpendicular to the plane of the layers is twice that,  $2\Gamma A$ , of the  $\beta$  polytype. In the plane of the layers (plane  $x\Gamma y$ ), the first Brillouin zone corresponds to a regular hexagon (dashed line in figure 3(a)). By analogy with the  $\beta$  polytype, we have called M and K the high symmetry points at the Brillouin zone edges in this plane, with  $2\Gamma M = (4\pi/a\sqrt{3})[1 + (a/c)^2/12] = 1.846 \text{ \AA}^{-1}$  [17].

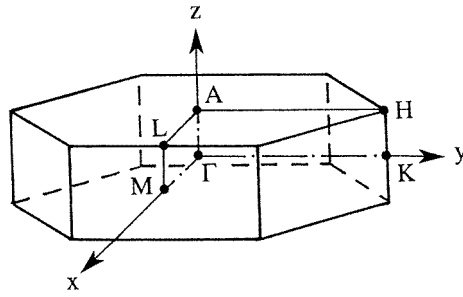


Figure 2. First Brillouin zone and high symmetry points of the  $\beta$  polytype of InSe.

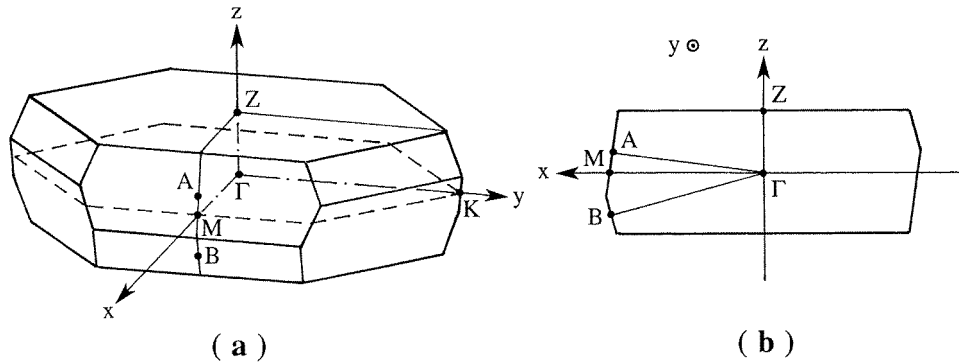


Figure 3. (a) First Brillouin zone of the  $\gamma$  polytype of InSe. (b) Contour of the  $\gamma$  polytype first Brillouin zone in the  $x\Gamma z$  plane.

#### 4. Dispersion curves in the plane of the layers

Examples of the valence band spectra obtained with the two photon energies of 29 and 48 eV at various emission angles are displayed in figures 4 and 5 for the  $\Gamma M$  and  $\Gamma K$  directions respectively. All the spectra are plotted against binding energy referred to the valence band edge  $E_{VB}$  defining the zero of energy.

We can see in figures 4 and 5 that the different structures of the spectra change somewhat with emission angle in both energy position and intensity. The changes in peak positions reflect the dispersion of the electronic states, while the intensity variations are attributed to the variations of the matrix elements involved in the optical transition [18]. When we compare the spectra obtained with a photon energy of 29 eV to those measured with 48 eV in the  $\Gamma M$  (figure 4) or  $\Gamma K$  (figure 5) direction, for the same emission angle, the intensities of the peaks are different. This is due to the variations of the matrix elements with photon energy. We can notice that there is a symmetry of the spectra about  $\theta_e = 0$ . This can be observed by comparing, for each photon energy in the  $\Gamma M$  (figure 4) and  $\Gamma K$  (figure 5) directions, the spectra recorded at an emission angle of  $-6^\circ$  and  $-2^\circ$  to those at  $6^\circ$  and  $2^\circ$  respectively.

To determine the dispersion curves in the plane of the layers, we have, for each peak of the spectra, read off its energy position and calculated the surface parallel component  $k_{\parallel}$  of the electron wave vector inside the solid using equation (1). We have then plotted the initial-state electron binding energy  $E_i$  against  $k_{\parallel}$ . The results are displayed in figure 6(a) for  $h\nu = 29$  eV along the  $\Gamma M$  direction, and in figure 6(b) for  $h\nu = 48$  eV along the  $\Gamma K$  direction. The binding

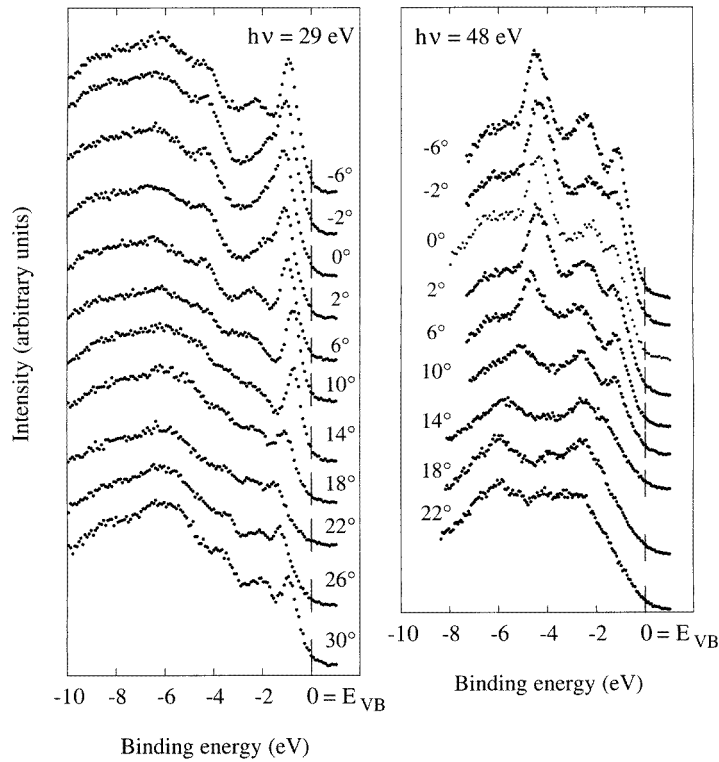


**Figure 4.** Evolution of the valence band spectra as a function of the emission angle along the  $\Gamma M$  azimuth for  $h\nu = 29$  eV and 48 eV. The binding energies are referred to the top of the valence band  $E_{VB}$ .

energies are referred to the valence band edge. The positions of the high symmetry points  $\Gamma$ , M and K are represented by solid lines in the case of the  $\gamma$  polytype and by dashed lines for the  $\beta$  polytype. In each direction, wave vectors well beyond the first Brillouin zone boundaries M and K are reached. The sequences of high symmetry points encountered in the extended zone scheme are  $\Gamma M \Gamma$  along the  $\Gamma M$  azimuth (figure 6(a)) and  $\Gamma K M K \Gamma$  along the  $\Gamma K$  azimuth (figure 6(b)).

In figures 6(a) and 6(b), four main groups of structures may be distinguished. They correspond to the four groups of bands that are predicted by calculations for  $\beta$ -InSe bulk material [9]. For convenience, we shall denote by A, B, C and D the different structures of figure 6 in order of increasing binding energy. The uppermost band A, around  $-1$  eV at  $k_{\parallel} = 0$ , corresponds to a bonding band of the In–In bond, perpendicular to the plane of the layers, involving 5s and 5p<sub>z</sub> orbitals of In that hybridize to Se 4p<sub>z</sub> orbitals. The group of structures B, around  $-2$  eV at  $k_{\parallel} = 0$ , corresponds to 4p<sub>x</sub> and 4p<sub>y</sub> orbitals of the Se atoms responsible for the covalent In–Se bond in the plane of the layers. The C and D bands, around  $-4.3$  eV and  $-6.3$  eV at  $k_{\parallel} = 0$  respectively, are the antibonding (C) and bonding (D) bands of the In–In bond involving In 5s orbitals that hybridize somewhat to the 5p<sub>z</sub> states of In.

In the extended zone scheme, we should have in the two directions  $\Gamma M \Gamma$  and  $\Gamma K M K \Gamma$  a mirror symmetry about the M point. Such a mirror symmetry is not obvious for the  $\Gamma K M K \Gamma$  direction (figure 6(b)) since the bands remain rather flat in the KM region. On the other hand, in the  $\Gamma M \Gamma$  direction (figure 6(a)), the experimental bands do display a mirror symmetry about

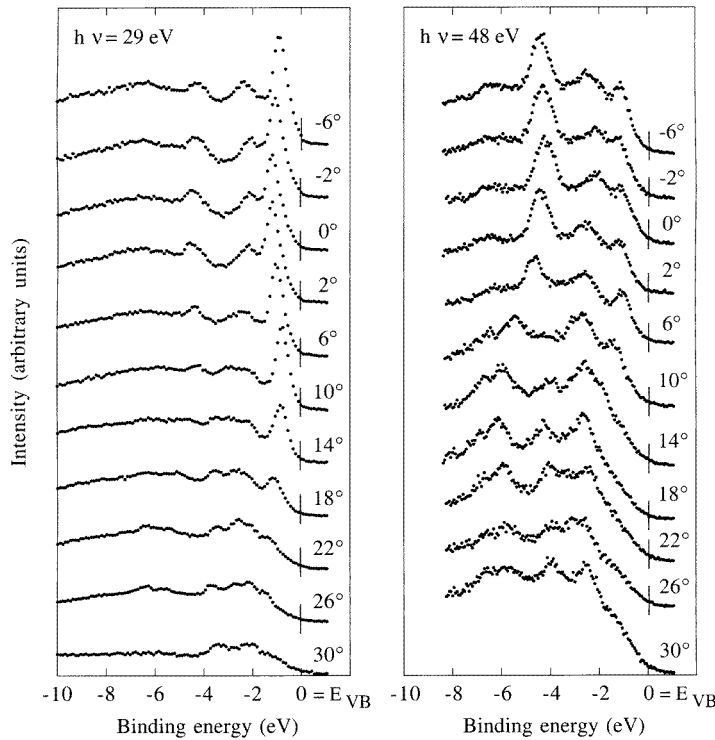


**Figure 5.** Evolution of the valence band spectra as a function of the emission angle along the  $\Gamma K$  azimuth for  $h\nu = 29$  eV and 48 eV. The binding energies are referred to the top of the valence band  $E_{VB}$ .

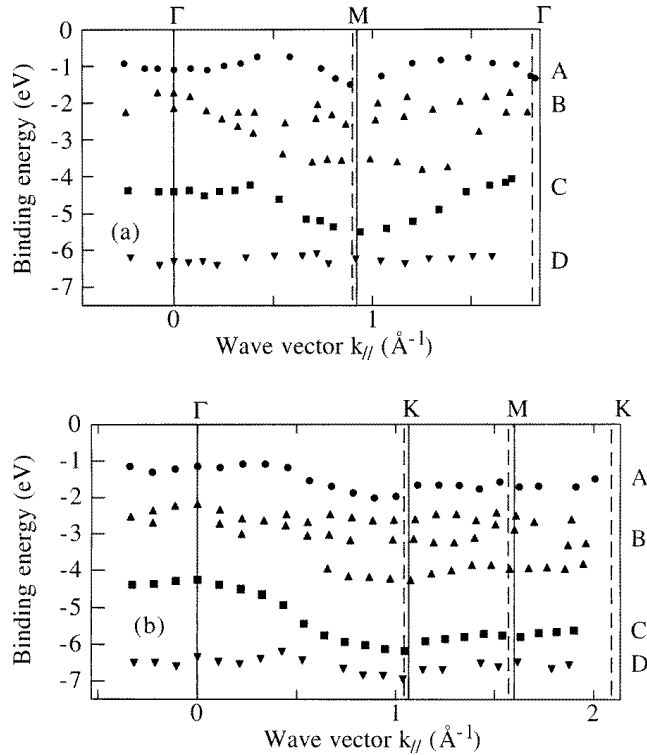
the M point. Although the difference is slight between the Brillouin zone dimensions, parallel to the layers, of the  $\beta$  and  $\gamma$  polytypes, this symmetry appears somewhat less satisfactory for the  $\beta$  polytype (dashed line) than for the  $\gamma$  polytype (solid line) especially for the A and C bands. These observations are consistent with the TEM results on the InSe epitaxial thin films.

Figure 7 represents the dispersion curves obtained in the reduced zone scheme using equation (3) with the parameters of the  $\gamma$  polytype ( $k_{BZ} = \Gamma M = 0.923 \text{ \AA}^{-1}$ ). This figure has been plotted with the results obtained at  $h\nu = 48$  eV except for B and D bands between M and  $\Gamma$  points that correspond to the photon energy of 29 eV. This has been done in order to obtain a band structure as complete as possible, the D band being absent at  $h\nu = 48$  eV between M and  $\Gamma$ , and some bands of the B group being observed only at  $h\nu = 29$  eV between M and  $\Gamma$ .

The experimental band structure of  $\beta$ -InSe bulk material has been determined from angle-resolved photoemission by Larsen *et al* [7] for the two symmetry directions  $\Gamma M$  and  $\Gamma K$ . On the whole, our results are quite similar to theirs concerning the existence of the various bands A to D. However, there are some differences for the A and C bands close to the  $\Gamma$  point. Indeed, in the two directions  $\Gamma M$  and  $\Gamma K$ , Larsen *et al* [7] have found that the uppermost band splits into two sub-structures around the  $\Gamma$  point. Such a splitting is also observed in the experimental points for the C band. We do not see such effects in the dispersion curves of our  $\gamma$  polytype thin film (figure 7).

Gomes da Costa *et al* [12] have calculated from first principles the band structure of InSe for the two polytypes  $\gamma$  and  $\beta$ . Their calculations, neglecting the spin-orbit interactions,





**Figure 6.** Experimental dispersion curves in the plane of the layers along the  $\Gamma M \Gamma$  direction for  $h\nu = 29$  eV (a) and along the  $\Gamma K M K$  direction for  $h\nu = 48$  eV (b). The origin of the binding energies is the top of the valence band. The solid lines at  $\Gamma$ ,  $K$  and  $M$  points correspond to the  $\gamma$  polytype in the extended zone scheme, and the dashed lines to the  $\beta$  polytype. A, B, C and D correspond to the groups of bands discussed in the text.

are reported for the high symmetry planes  $\Gamma K H A$  and  $\Gamma M L A$  (figure 2) in the case of the  $\beta$  polytype, and along the  $\Gamma A$  and  $\Gamma B$  directions of the first Brillouin zone (figure 3) for the  $\gamma$  polytype. These authors have found that the electronic structures of the two polytypes are quite similar in the sense that the different electronic levels A, B, C and D are present in each of them. However, there are twice as many bands for the  $\beta$  polytype as compared to the  $\gamma$  polytype since its primitive cell extends over two layers while that of the  $\gamma$  polytype includes only one layer. As a consequence, some bands (A, C and D) appear split into two levels around the  $\Gamma$  point in the case of the  $\beta$  polytype [12]. This is a consequence of zone folding in the direction perpendicular to the layers in going from  $\gamma$  to  $\beta$  polytype. Thus, the splitting of the states observed by Larsen *et al* around the  $\Gamma$  point is characteristic of the  $\beta$  polytype they have studied. Conversely, the absence of splitting, as we observe (figure 7) is consistent with the fact that the  $\gamma$  polytype has developed in our InSe thin film.

In figure 8 we compare our experimental results obtained for  $h\nu = 29$  eV along  $\Gamma M$  in the reduced zone scheme using the  $\gamma$  polytype parameters to the band structure of  $\gamma$ -InSe calculated by Gomes da Costa *et al* [12]. Figure 8 has been obtained by placing the experimental origin of energy onto that of the theoreticians. The calculated band structure of  $\gamma$ -InSe is given for the  $\Gamma A$  and  $\Gamma B$  directions (bottom axes) that are not rigorously equivalent to the  $\Gamma M$  direction (top axes) along which we have carried out our measurements. One should notice that the

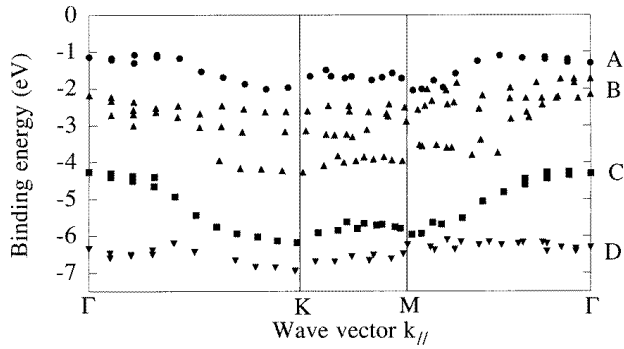


**Figure 7.** Experimental dispersion curves in the reduced zone scheme  $\Gamma\text{KMG}$  obtained with  $h\nu = 48$  eV and with the  $\gamma$  polytype parameters. The B and D bands between the M and  $\Gamma$  points have been obtained with  $h\nu = 29$  eV. The origin of the binding energies is the top of the valence band.

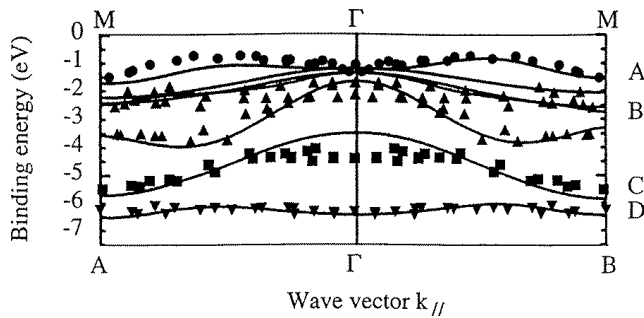


**Figure 8.** Comparison between the experimental dispersion curves in the reduced zone scheme along  $\Gamma\text{M}$  and the calculations of Gomes da Costa *et al* [12] along  $\Gamma\text{A}$  and  $\Gamma\text{B}$ . The symbols correspond to the experimental data from the InSe thin film. The smooth curves are the theoretical results for  $\gamma$ -InSe without spin-orbit interactions, reproduced from [12].

theoretical dispersion curves along  $\Gamma\text{A}$  and  $\Gamma\text{B}$  are very similar to each other although these two directions are not equivalent. The  $\Gamma\text{M}$  azimuth, which is in the plane of the layers, is intermediate between  $\Gamma\text{A}$  and  $\Gamma\text{B}$  (figure 3(a)), and we would expect the dispersion curves along  $\Gamma\text{M}$  to be close to those along  $\Gamma\text{A}$  and  $\Gamma\text{B}$ , the only ones which we can compare to.

Figure 8 clearly shows the very good agreement between experimental and calculated bands of  $\gamma$ -InSe. Except the C band for which there is a shift of about 1 eV at  $\Gamma$  between experiment and calculation, the experimental and calculated energy positions, in particular at  $\Gamma$  and at the zone boundaries, agree in a way all the more remarkable since we did not need to adjust the top of the valence band. Although the calculation predicts a more important dispersion than what we observe for the C band, the sign and extent of energy dispersions are in good agreement for all the other bands. We can see that there is an apparently better agreement between the experimental dispersion curves along  $\Gamma\text{M}$  and the calculated ones for  $\Gamma\text{B}$ , in particular concerning the A and B bands at zone boundaries. Although this may be fortuitous, one should note that the projection of  $\Gamma\text{B}$  onto the  $\Gamma x$  axis is  $\Gamma\text{M}$ , while this is not the case for  $\Gamma\text{A}$  (figure 3(b)).

As we have pointed out, the C band at the  $\Gamma$  point is observed experimentally at  $-4.3$  eV whereas it is found theoretically at  $-3.5$  eV for  $\gamma$ -InSe (figure 8). We do not understand the

origin of this discrepancy which is far beyond the experimental uncertainty. It appears the more surprising as the agreement is very good for the other states. As mentioned previously, the A, C and D bands split at the zone centre when going from the  $\gamma$  to the  $\beta$  polytype [12]. The theoretical states of the  $\gamma$  polytype correspond to the deeper state of the associated doublet in the  $\beta$  polytype for the A and D bands, and to the upper one for the C band. However, the experimental states of our  $\gamma$  polytype thin film correspond to the theoretical deeper state of the associated doublets in  $\beta$  polytype for all three bands.

There is another disagreement between the experimental band structure of InSe and the calculated one in figure 8. It concerns the existence of an experimental state at  $-2.3$  eV at the zone centre  $\Gamma$  which does not correspond to any theoretical state either of the  $\gamma$  polytype or of  $\beta$ , but which has also been observed by Larsen *et al* [7] in their experimental study of the  $\beta$  polytype. The calculation for the  $\gamma$  polytype to which we compare our results neglects spin-orbit interactions. But the latter have non-negligible effects on the band structure of  $\gamma$ -InSe [12] by splitting the two top valence bands at  $\Gamma$  as well as each of the two doubly degenerate second and third valence bands at the zone boundary Z. As a consequence, some states are pulled away from the valence band edge. The theoretical results taking into account spin-orbit interactions [12] are given along the  $\Gamma$ A,  $\Gamma$ B and  $\Gamma$ Z directions but only down to  $-1.7$  eV from the top of the valence band. The dispersion curves along  $\Gamma$ Z reveal a state which would reach  $\Gamma$  farther away from the valence band edge. This suggests that this explanation of the observed disagreement would be correct.

## 5. Dispersion curves along the normal to the plane of the layers

It had been assumed for a while that the electronic states of layered compounds have almost no dispersion perpendicular to the plane of the layers [19–21]. However, quite soon, theoretical and experimental studies showed the coexistence of states with two-dimensional character and states with three-dimensional character [22]. In order to test the importance of the dispersion along the normal to the plane of the layers in the case of  $\gamma$ -InSe, we have measured the valence band spectrum at normal emission ( $\theta_e = 0$ ) for different photon energies. Figure 9 displays a set of valence band spectra obtained at various photon energies between 29 and 60 eV. The spectra are plotted against binding energy referred to the valence band edge. As we can see, the different structures of the spectra change in energy position and in intensity with photon energy. The intensity variation is attributed to the variations of the matrix element of the optical transition with photon energy. The change in energy position shows that there is a dispersion of the electronic states perpendicularly to the plane of the layers.

For each structure, we have calculated the normal component  $k_{\perp}$  of the electron wave vector inside the solid using equation (4) with the  $\gamma$  polytype parameters  $k_{BZ} = \Gamma Z = 0.377 \text{ \AA}^{-1}$ . To determine the inner potential  $V_0$  involved in equation (4) and which is not easily measurable, we have tested several values between the top and the bottom of the valence band. We have then adopted a value of  $-11.85$  eV, close to the bottom of the valence band, which seems to give, for the A and C bands that are in principle the most dispersive ones [22], the expected periodicity in the extended zone scheme for the  $\gamma$  polytype. Our dispersion curves in the reduced zone scheme along  $\Gamma$ Z are presented in figure 10 and compared to the calculation without spin-orbit interaction of Gomes da Costa *et al* for  $\gamma$ -InSe [12]. The top of the valence band has been taken as the origin of binding energies. In figure 10 the experimental valence band edge coincides with the theoretical one.

The overall agreement between calculation and experiment along  $\Gamma$ Z (figure 10) appears quite satisfactory although it does not seem as good as parallel to the layers (figure 8). This difference may arise from the presence of the inner potential as a parameter in equation (4)

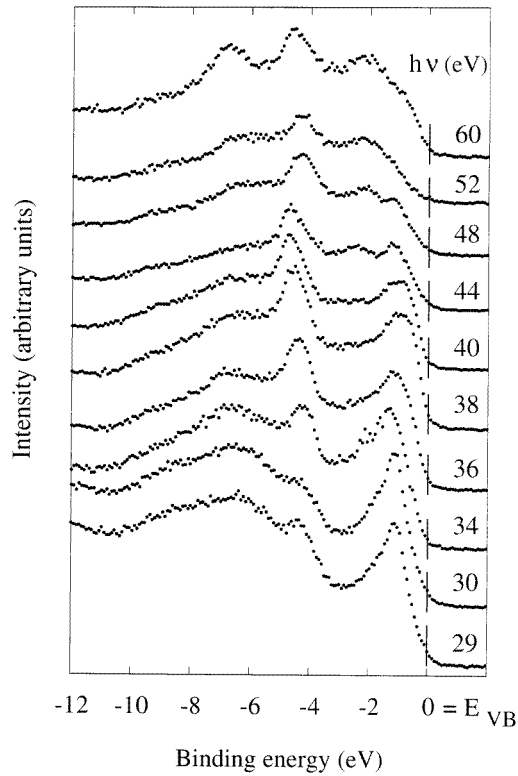


**Figure 9.** Evolution of the valence band spectra at normal emission as a function of photon energy. The binding energies are referred to the top of the valence band  $E_{VB}$ .

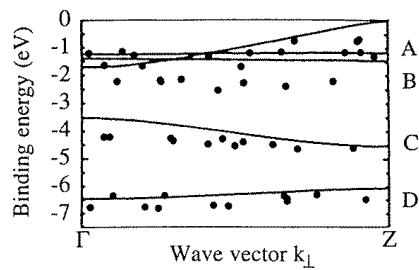


**Figure 10.** Comparison between the experimental dispersion curves in the reduced zone scheme along  $\Gamma Z$ , the normal to the plane of the layers, and the calculations of Gomes da Costa *et al* [12]. The symbols correspond to the experimental data from the InSe thin film. The smooth curves are the theoretical results for  $\gamma$ -InSe without spin-orbit interactions, reproduced from [12].

used to determine  $k_{\perp}$ . Aside from a slight downward shift, by 0.2–0.3 eV, of the experimental points with respect to the theoretical curve (figure 10), the experimental dispersion for the D band and that for the C band towards the Brillouin zone edge agree quite well with theory. Also the existence of dispersionless B bands is observed.

The C band extrapolated at  $\Gamma$  gives a state at  $-4.2$  eV, much deeper than the theoretical limit at the zone centre. This discrepancy has been pointed out in the previous section. Among

the B bands, which involve the In–Se covalent bond in the plane of the layer, one is observed at  $-2.3$  eV. This state, at  $\Gamma$ , has been discussed previously, and it has been related to spin–orbit interactions. However, nothing in the theoretical results [12] suggests it exists throughout the Brillouin zone in the  $\Gamma Z$  direction.

For the A band, the calculated dispersion along  $\Gamma Z$  is found to be much larger than the experimental one. It should be noted that the calculated A band reaches the top of the valence band at the zone boundary Z, while experimentally we do not find points in this part of the dispersion curves. The top of the valence band corresponds to a non-bonding lone-pair  $p_z$  orbital on Se and a  $\sigma_z$  bonding orbital of the In–In bond [12]. It has then a  $p_z$  character perpendicular to the plane of the layers. Our experimental conditions of measurements, with an angle of incidence of light of  $22.5^\circ$  and a polarization in the plane of incidence, were not favourable to excite such an electronic state.

## 6. Conclusion

Angle-resolved ultraviolet photoelectron spectroscopy using synchrotron radiation was used to determine the experimental band structure of an epitaxial thin film of the layered semiconductor InSe. Our results are consistent with the fact that this thin film grown on Si(111)1  $\times$  1-H substrate crystallizes as the  $\gamma$  polytype. This implies a remarkable control of the growth which requires a smooth substrate at the atomic scale, and stringent growing conditions since the In–Se phase diagram, with several definite compounds, is quite complex. The good quality of the film enabled a reliable determination of the dispersion curves along directions parallel to the plane of the layers as well as perpendicular to it. The good overall agreement between theory developed for bulk InSe of  $\gamma$  polytype, and experiment performed on a InSe film, about eight layers thick, in which the  $\gamma$  phase prevails, indirectly confirms that the outer layers probed in the measurements are relaxed to bulk InSe parameters. A few apparent discrepancies with theory have been pointed out which might be related to spin–orbit interactions. To our knowledge, this is the first time that experimental dispersion curves of a  $\gamma$  phase III–VI layered compound have been reported.

## Acknowledgments

The authors would like to gratefully thank the whole staff of line SA73 and of the PHD experimental station for their very efficient help in running the experiments at LURE. They are also very much obliged to A Köebel and Y Zheng of the Laboratoire de Minéralogie Cristallographie for letting them publish the TEM results of figure 1.

## References

- [1] Kuhn A, Chevy A and Chevalier R 1975 *Phys. Status Solidi* a **31** 469
- [2] Le Thanh V, Eddrief M, Sébenne C A, Sacuto A and Balkanski M 1994 *J. Crystal Growth* **135** 1
- [3] Amimer K 1998 *Thesis* Université Montpellier II, Montpellier, France
- [4] Köebel A, Zheng Y, Pétrouff J F, Eddrief M, Le Thanh V and Sébenne C 1995 *J. Crystal Growth* **154** 269
- [5] Köebel A 1997 *Thesis* Université Denis Diderot–Paris VII, Paris, France
- [6] Zheng Y 1999 private communication
- [7] Larsen P K, Chiang S and Smith N V 1977 *Phys. Rev. B* **15** 3200
- [8] McCann J V and Murray R B 1977 *J. Phys. C: Solid State Phys.* **10** 1211
- [9] Doni E, Girlanda R, Grasso V, Balzarotti A and Piacentini M 1979 *Nuovo Cimento B* **51** 154
- [10] Robertson J 1979 *J. Phys. C: Solid State Phys.* **12** 4777
- [11] Depeursinge Y 1981 *Nuovo Cimento B* **64** 111

- [12] Gomes da Costa P, Dandrea R G, Wallis R F and Balkanski M 1993 *Phys. Rev. B* **48** 14 135
- [13] Seah M P and Dench W A 1979 *Surf. Interface Anal.* **1** 2
- [14] Proix F, Panella V, El Monkad S, Glebov A, Lacharme J P, Eddrief M, Amimer K, Sébenne C A and Toennies J P 1998 *Eur. Phys. J. B* **5** 919
- [15] El Monkad S, Eddrief M, Lacharme J P, Amimer K and Sébenne C A 1996 *Surf. Sci.* **352/354** 833
- [16] For the parameters of the  $\beta$  polytype, we have used  $a = 4.005 \text{ \AA}$  and  $c = 8.32 \text{ \AA}$  from Popovic S 1973 *J. Appl. Crystallogr.* **6** 122
- [17] For the parameters of the  $\gamma$  polytype, we have used  $a = 4.0046 \text{ \AA}$  and  $c = 8.32 \text{ \AA}$  from Nagpal K C and Ali S Z 1975 *Acta Crystallogr. A* **31** S67
- [18] Cardona M and Ley L (eds) 1978 *Photoemission in Solids I (Topics in Applied Physics 26)* (Berlin: Springer)
- [19] Ottaviani G, Canali C, Nava F, Schmid P H, Mooser E, Minder R and Zschokke I 1974 *Solid State Commun.* **14** 933
- [20] Schlüter M, Camassel J, Kohn S, Voitchovsky J P, Shen Y R and Cohen M L 1976 *Phys. Rev. B* **13** 3534
- [21] Schlüter M 1973 *Nuovo Cimento B* **13** 313
- [22] Larsen P K, Schlüter M and Smith N V 1977 *Solid State Commun.* **21** 775